An intermolecular G-quadruplex as the basis for GTP recognition in the class V–GTP aptamer

AMIR H. NASIRI,[1] JAN PHILIP WURM,[1] CARINA IMMER, ANNA KATHARINA WEICKHMANN, and JENS WÖHNERT

Institute of Molecular Biosciences and Center for Biomolecular Magnetic Resonance (BMRZ), Johann-Wolfgang-Goethe-University Frankfurt, 60438 Frankfurt, Germany

ABSTRACT

Many naturally occurring or artificially created RNAs are capable of binding to guanine or guanine derivatives with high affinity and selectivity. They bind their ligands using very different recognition modes involving a diverse set of hydrogen bonding and stacking interactions. Apparently, the potential structural diversity for guanine, guanosine, and guanine nucleotide binding motifs is far from being fully explored. Szostak and coworkers have derived a large set of different GTP-binding aptamer families differing widely in sequence, secondary structure, and ligand specificity. The so-called class V–GTP aptamer from this set binds GTP with very high affinity and has a complex secondary structure. Here we use solution NMR spectroscopy to demonstrate that the class V aptamer binds GTP through the formation of an intermolecular two-layered G-quadruplex structure that directly incorporates the ligand and folds only upon ligand addition. Ligand binding and G-quadruplex formation depend strongly on the identity of monovalent cations present with a clear preference for potassium ions. GTP binding through direct insertion into an intermolecular G-quadruplex is a previously unobserved structural variation for ligand-binding RNA motifs and rationalizes the previously observed specificity pattern of the class V aptamer for GTP analogs.

Keywords: RNA structure; GTP; aptamer; NMR; G-quadruplex; ligand binding

INTRODUCTION

Many RNA structural motifs are capable of binding to guanine, guanosine, or guanine nucleotides and their derivatives with high specificity and affinity. These motifs have been found not only in naturally occurring functional RNAs such as ribozymes or riboswitches but also in artificial RNAs derived from SELEX experiments. They vary widely in their structures and ligand recognition modes. In all structurally characterized examples, hydrogen bonding and stacking interactions play an important role for ligand recognition and in general the guanine base is a major determinant for ligand recognition. One classic example for an RNA interacting with a guanine-derived ligand is the self-splicing group I intron (Cech et al. 1981), which binds its cofactor guanosine through a base-pairing interaction between the Hoogsteen edge of a conserved guanine nucleotide and the Watson-Crick face of the guanosine cofactor (Adams et al. 2004). Two hydrogen bond donor groups from the ligand guanosine, the N2 amino and the N1 imino group, form two hydrogen bonds with the N7 nitrogen and the C6 carbonyl group as acceptors, respectively. The guanine (Mandal et al. 2003) and deoxyguanosine (Kim et al. 2007) sensing riboswitches bind guanine or deoxyguanosine through a Watson-Crick base-pairing interaction with a cytidine residue (Batey et al. 2004; Serganov et al. 2004; Noeske et al. 2005; Edwards and Batey 2009; Pikovskaya et al. 2011; Wacker et al. 2011). An additional base-pairing interaction engages the sugar edge of the ligand. Furthermore, there are two structurally distinct classes of cyclic-di-GMP-sensing riboswitches (Sudarsan et al. 2008; Lee et al. 2010). They recognize both guanine base moieties of their ligand through a variety of non-Watson-Crick interactions (Kulshina et al. 2009; Smith et al. 2009, 2011). Very recently, Liu and coworkers reported the widespread occurrence of GTP-binding DNA and RNA motifs encoded in the genomes of chicken and human which bind to GTP with equilibrium dissociation constants (K_D's) > 100 μM (Curtis and Liu 2013). The sequences of some of these motifs and CD-spectroscopic data suggested that many of them could fold into G-quadruplex structures. An analysis of GTP-analog binding to these motifs

[1]**Joint first authors.**

Corresponding author: woehnert@bio.uni-frankfurt.de

Article published online ahead of print. Article and publication date are at http://www.rnajournal.org/cgi/doi/10.1261/rna.058909.116.

suggested that the ligand GTP might be an integral part of their G-quadruplex structure.

GTP has also been a target for raising artificial RNA aptamers in SELEX experiments. In particular, the work by the Szostak group (Davis and Szostak 2002; Huang and Szostak 2003; Carothers et al. 2004) showed that a large number of structurally highly diverse RNA motifs are capable of binding to GTP with a wide range of affinities and differences in specificity.

However, from this multitude of SELEX-derived GTP-aptamer families only one class has been analyzed structurally so far (Carothers et al. 2006a). The so-called class I GTP aptamer contains 41 nucleotides (nt) and binds GTP with a K_D of 74 nM. Its NMR-solution structure revealed an internal bulge with an intricate tertiary structure featuring a number of noncanonical base-pairing interactions bound by two canonical A-form helical stems. GTP is recognized through hydrogen bonding interactions of the N7 nitrogen and the C6 carbonyl group on its Hoogsteen face with the N1 imino group and the N2 amino group on the Watson-Crick face of a guanine nucleotide of the aptamer, respectively. Importantly, only the base portion of the nucleotide is interacting with the aptamer RNA while the ribose and the triphosphate moieties do not contribute to specific intermolecular interactions.

We were interested in understanding the GTP recognition mode of the class V aptamer from the same series of GTP-binding aptamers (Carothers et al. 2004). This aptamer was reported to have a very high affinity for GTP with a K_D of 17 nM. A complex secondary structure with three A-form helical stem elements separated by two asymmetric internal bulges containing a number of highly conserved nucleotides was suggested (Fig. 1A) based on the analysis of sequence conservation. So far, no crystal structure of the aptamer/GTP complex is available. A full high-resolution structure determination by solution NMR spectroscopy is rendered difficult by the larger size of this molecule (68 nt) leading to significant signal overlap and more importantly by unfavorable internal dynamics resulting in line broadening and preventing signal assignments and the collection of a sufficient amount of NOE distance constraints. However, the NMR experiments we describe here unequivocally demonstrate that the ligand GTP is bound by this aptamer through the ligand-induced formation of a two-layered G-quadruplex into which GTP is directly incorporated. Nucleotides from both asymmetric internal bulges contribute to the formation of the G-quadruplex structure. Thus, the GTP–class V aptamer joins the surprisingly short list of small molecule binding RNA aptamers that use G-quadruplex elements as integral parts of their ligand-binding sites (Lauhon and Szostak 1995; Phan et al. 2011; Dolgosheina et al. 2014; Huang et al. 2014; Warner et al. 2014). To our knowledge, it is the first verified example for specific ligand recognition by an RNA through the formation of an intermolecular G-quadruplex structure.

RESULTS AND DISCUSSION

The class V aptamer binds GTP via a non-Watson-Crick interaction

In order to probe the interaction between GTP and the class V aptamer, we produced the aptamer RNA by in vitro transcription with T7-RNA polymerase using either unlabeled,

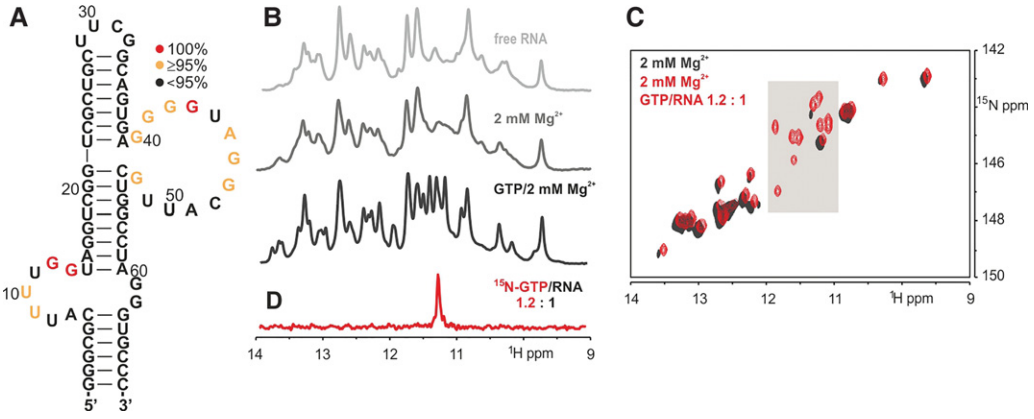

FIGURE 1. The GTP–class V aptamer binds GTP through non-Watson-Crick interactions. (*A*) Secondary structure of the class V–GTP-binding aptamer as predicted by Szostak and coworkers (Carothers et al. 2004). Based on the previously reported sequences of this aptamer, the degree of nucleotide conservation was calculated and is indicated by different colors with completely conserved nucleotides shown in red and nucleotides conserved in >95% of the reported sequences shown in orange. (*B*) 1D-^{1}H imino proton spectra in potassium phosphate buffer for the GTP–class V aptamer in its free form (*top*), in the presence of 2 mM Mg^{2+} (*middle*), and in the presence of 2 mM Mg^{2+} and 1.2 eq of GTP (*bottom*). (*C*) Overlay of ^{1}H,^{15}N-HSQC spectra of the ^{15}N-guanine-labeled class V aptamer RNA in the presence of 2 mM Mg^{2+} (black) and in the presence of 2 mM Mg^{2+} and 1.2 eq of ^{15}N,^{13}C-labeled GTP (red). The spectra are slightly displaced with respect to each other. A gray box highlights the area where a number of guanine imino group signals appear only upon addition of the ligand GTP. (*D*) The 1D slice of a ^{1}H,^{15}N-HSQC spectrum recorded with a sample consisting of unlabeled RNA and ^{15}N-labeled GTP reveals the imino group signal of the bound GTP with a chemical shift of 11.2 ppm outside the range typically found for guanine imino protons in Watson-Crick base pairs.

^{15}N-labeled, or ^{15}N,^{13}C-labeled GTP and unlabeled ATP, CTP, and UTP, respectively. In comparison to the sequence reported previously (Carothers et al. 2004), our version of the aptamer contains a slight modification in the lower helix in order to optimize transcription yields by avoiding stretches of the same nucleotide longer than three nucleotides (Fig. 1A). 1D-^{1}H-NMR spectra recorded for the free RNA in potassium phosphate buffer (25 mM KPO_4, pH 6.3, 50 mM KCl) at 10°C (Fig. 1B, top) showed numerous signals for imino protons with chemical shifts typical for guanine and uridine residues in both Watson-Crick (~12.0–14.5 ppm) and noncanonical base pairs (<12.0 ppm). There are four G:U wobble base pairs predicted to be present in the secondary structure of the class V aptamer explaining the presence of at least some of the imino proton signals with chemical shifts <12.0 ppm. Importantly, another imino proton signal is observable at 9.6 ppm demonstrating that the stable apical UUCG-tetraloop folds as expected from the predicted secondary structure (Varani et al. 1991). However, even when taking into account the size of the class V aptamer (68 nt), the observable imino proton signals are very broad. Thus, the free class V aptamer apparently exists as an ensemble of multiple interconverting structures resulting in exchange broadening of the corresponding NMR signals. Addition of Mg^{2+} ions, which were present throughout the selection procedure for this aptamer, does not lead to major changes in the appearance of the imino proton spectrum (Fig. 1B, middle). In contrast, the addition of one molar equivalent of GTP results in dramatic changes of the imino proton spectrum of the class V aptamer (Fig. 1B, bottom), confirming that GTP binds to the RNA as expected. The further addition of GTP does not induce additional changes in the spectrum in agreement with the formation of a 1:1 GTP-RNA complex in slow exchange on the NMR time scale. GTP binding results in a sharpening of all imino proton signals as well as in the appearance of additional imino proton signals with chemical shifts in the range between ~11 and 12 ppm. Most of these newly appearing imino proton signals belong to guanine nucleotides as demonstrated by the comparison of ^{1}H,^{15}N-HSQC spectra recorded for the free ^{15}N-G-labeled RNA and the RNA-GTP complex (Fig. 1C) in the presence of Mg^{2+}. Thus, GTP binding induces the formation of a single, well-defined tertiary structure of the class V aptamer. The addition of GTP to the RNA in the absence of Mg^{2+} does not lead to changes in the imino proton spectra, demonstrating that complex formation is strictly Mg^{2+} dependent (Supplemental Fig. 1). In agreement with previous reports (Carothers et al. 2006b) that 6-Thio-GTP does not bind to the class V aptamer, the addition of even a large excess of 6-Thio-GTP does not induce spectral changes (Supplemental Fig. 2). To gain insights into the GTP recognition mode of the class V aptamer, we recorded 1D- and 2D-^{1}H,^{15}N-HSQC spectra for a complex formed between ^{15}N-labeled GTP and unlabeled RNA (Fig. 1D; Supplemental Fig. 3). In these experiments, a single imino group resonance is observed for the bound GTP while no imino signal is observable for free GTP due to fast chemical exchange of the imino proton with the bulk solvent. Thus, in the bound state, the GTP imino proton is protected against exchange by hydrogen bonding interactions with the RNA. The ^{1}H chemical shift for the imino proton of the bound GTP (11.2 ppm) does not conform to a Watson-Crick base-pairing interaction between ligand and aptamer (Fürtig et al. 2003). Furthermore, no correlation peaks of the GTP imino group with other nitrogens were observed in HNN-COSY experiments (Dingley and Grzesiek 1998; Wöhnert et al. 1999) with ^{15}N-labeled RNA bound to ^{15}N-labeled GTP. Taken together, the absence of correlation peaks in the HNN-COSY experiments and the observed imino proton chemical shift suggest that the hydrogen bond acceptor for the GTP imino group is most likely an oxygen containing functional group of the RNA (Fürtig et al. 2003).

GTP binding to the class V aptamer is dependent on the identity of the monovalent cation

Interestingly, GTP binding to the class V aptamer not only depends on the presence of Mg^{2+} ions but also on the presence of potassium ions. When the NMR-titration experiments were repeated in a buffer containing 50 mM Bis-Tris, pH 6.3, 5 mM $MgCl_2$ and no potassium ions, no GTP binding was observed. The GTP-RNA complex only formed upon the addition of KCl to this buffer (Supplemental Fig. 4). Furthermore, in titrations of the class V aptamer with GTP in a sodium phosphate buffer (25 mM $NaPO_4$, pH 6.3, 50 mM NaCl, 2 mM $MgCl_2$) of equivalent ionic strength, only minor changes were observed in the imino proton spectra of the RNA even upon addition of an excess of GTP (Fig. 2A). In particular, no new imino proton signals appear in the chemical shift region between ~11 and 12 ppm and all signals already present in this spectral region in spectra of the free RNA can be assigned to imino protons of nucleotides in G:U wobble base pairs (Supplemental Fig. 5). Furthermore, in titration experiments with ^{15}N-labeled GTP and unlabeled RNA, the 1D-^{1}H,^{15}N-HSQC spectra in sodium phosphate buffer showed only a weak and broad signal for the imino proton of bound GTP (Fig. 2B). Taken together, this shows that in the presence of sodium, the monovalent cation GTP binds much weaker to the class V aptamer than in the presence of potassium ions, and GTP does not induce tertiary folding of the aptamer RNA. In order to explore the relationship between monovalent cation identity and the binding affinity of the class V aptamer for GTP quantitatively, the GTP affinity was measured using isothermal titration calorimetry in buffer conditions with equivalent ionic strengths. In the presence of potassium ions, a K_D of the aptamer for GTP of 70 nM was found (Fig. 2C), which is similar to the K_D reported previously under slightly different buffer conditions (Carothers et al. 2004). No GTP binding was observed by ITC in the presence of sodium or lithium ions (Fig. 2C; Supplemental Fig. 6). On the other hand, in the presence

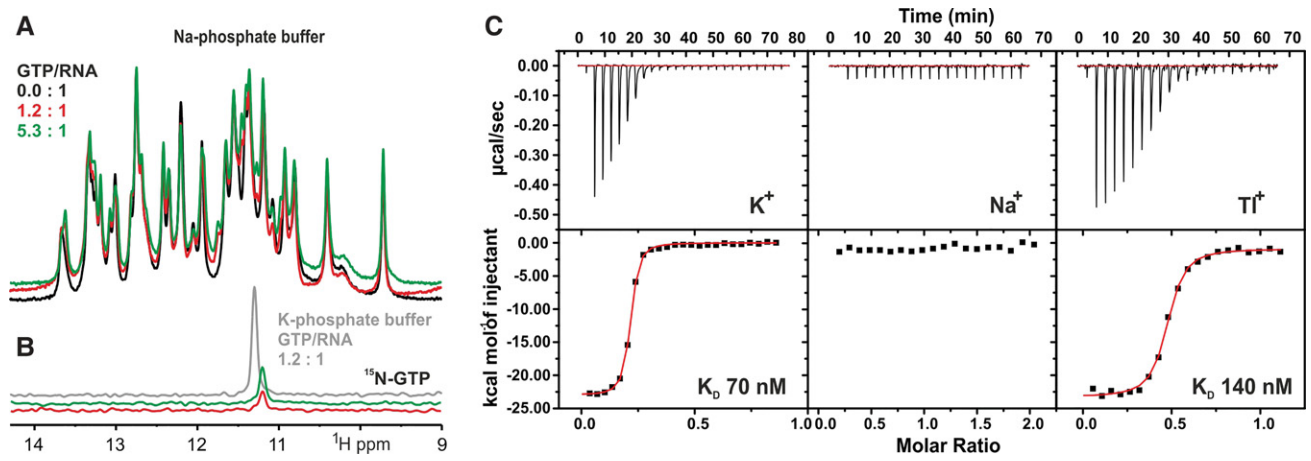

FIGURE 2. GTP binding to the class V aptamer RNA depends on the identity of the monovalent cations. (*A*) Overlay of 1D-^{1}H imino proton spectra of the GTP–class V RNA in a buffer containing 25 mM $NaPO_4$, 50 mM NaCl, 2 mM Mg^{2+} in the absence of GTP (black) and in the presence of 1.2 (red), and 5.3 eq of GTP. In contrast to the observations in the equivalent potassium phosphate buffer, ligand addition induces only minor changes in the spectra. (*B*) 1D slices of ^{1}H,^{15}N-HSQC spectra recorded for samples containing unlabeled RNA and 1.2 (red) or 5.3 eq (green) of ^{15}N-labeled GTP. Only a weak imino group signal corresponding to bound GTP is observed in comparison to the corresponding signal observed in potassium phosphate buffer (gray). (*C*) ITC thermograms and derived binding curves for GTP binding to the class V aptamer RNA in buffers of equivalent ionic strengths containing potassium, sodium, or thallium ions.

of thallium ions, the K_D for GTP was only slightly diminished (140 nM) (Fig. 2C), while in a buffer containing ammonium ions the GTP affinity is significantly lowered (3.1 µM) (Supplemental Fig. 6) in comparison to the potassium ion containing buffer. However, NMR spectra of the GTP–class V aptamer complex in a buffer containing 50 mM ammonium chloride show that an RNA-ligand complex is formed, which is in slow exchange on the NMR time scale, and a sharp signal is observable for the imino proton of the bound GTP (Supplemental Fig. 7). Thus, the affinity of the class V aptamer for GTP is highest in the presence of those monovalent ions that have ionic radii closely similar to potassium ions. Specific binding of RNAs to potassium ions has been reported before, e.g., for the *Tetrahymena* group I intron P4-P6 domain (Basu et al. 1998) and the 56 nt RNA domain that binds to bacterial ribosomal protein L11 (Conn et al. 2002). In the P4-P6 domain structure, the potassium binding site is located underneath an A:A platform. In the L11-binding RNA, a potassium ion is deeply buried in a specific binding pocket formed by a complex RNA tertiary structure stabilizing a three-way junction. Similar to our observations for the class V aptamer, the potassium ion can be replaced in both cases by thallium ions as demonstrated by X-ray crystallography (Basu et al. 1998; Conn et al. 2002). The L11-binding RNA domain also folds in the presence of ammonium ions, whereas sodium ions are much less effective in stabilizing this structure (Wang et al. 1993). However, another classic example for differential stabilization of RNA structures by different monovalent cations is G-quadruplexes. It has been demonstrated for both DNA- and RNA-G-quadruplex-containing structures that potassium ions are more effective than sodium or lithium ions in stabilizing these structures (e.g., Kim et al. 1991) but can be replaced by thallium (Basu et al. 2000; Gill et al. 2005, 2006) or ammonium ions (e.g., Hud et al. 1998, 1999; Podbevsek et al. 2007).

In G-quadruplexes, the guanine nucleotides bind to each other via interactions between the Watson-Crick edge of one nucleotide and the Hoogsteen edge of the second nucleotide (Fig. 3A). In this interaction, a G imino proton forms a hydrogen bond with the O6 carbonyl group, and a G amino group hydrogen binds to an N7 nitrogen. Due to the hydrogen bonding interactions of imino protons with oxygen containing acceptor groups, the imino proton signals of guanine nucleotides in G-quadruplexes are found between ~11 and 12 ppm (Jin et al. 1990; Wang et al. 1991a,b; Smith and Feigon 1992). Notably, the imino proton chemical shifts of the ligand GTP as well as a number of the imino protons of the RNA, which become only detectable upon GTP binding, have chemical shifts in exactly this region. Furthermore, the dependence of GTP binding on the identity of monovalent cations and the discrimination against 6-Thio-GTP binding are suggestive of the formation of an intermolecular G-quadruplex structure upon GTP binding to the class V aptamer where the GTP is directly incorporated into the quadruplex.

G-quadruplex formation gives rise to typical NOE patterns including the imino, amino, and aromatic H8 protons of the guanine nucleotides, which are part of this quadruplex (Jin et al. 1992; Smith and Feigon 1992; Macaya et al. 1993). In particular, there are NOEs between neighboring imino groups, between H8 and imino as well as between H8 and amino groups (Fig. 3A). Such NOEs are observable upon GTP binding to the class V aptamer in 2D-^{1}H,^{1}H-NOESY experiments with unlabeled RNA or in ^{13}C-edited NOESY-HSQC experiments with ^{13}C,^{15}N-G-labeled RNA for some of the imino groups with signals in the chemical shift region

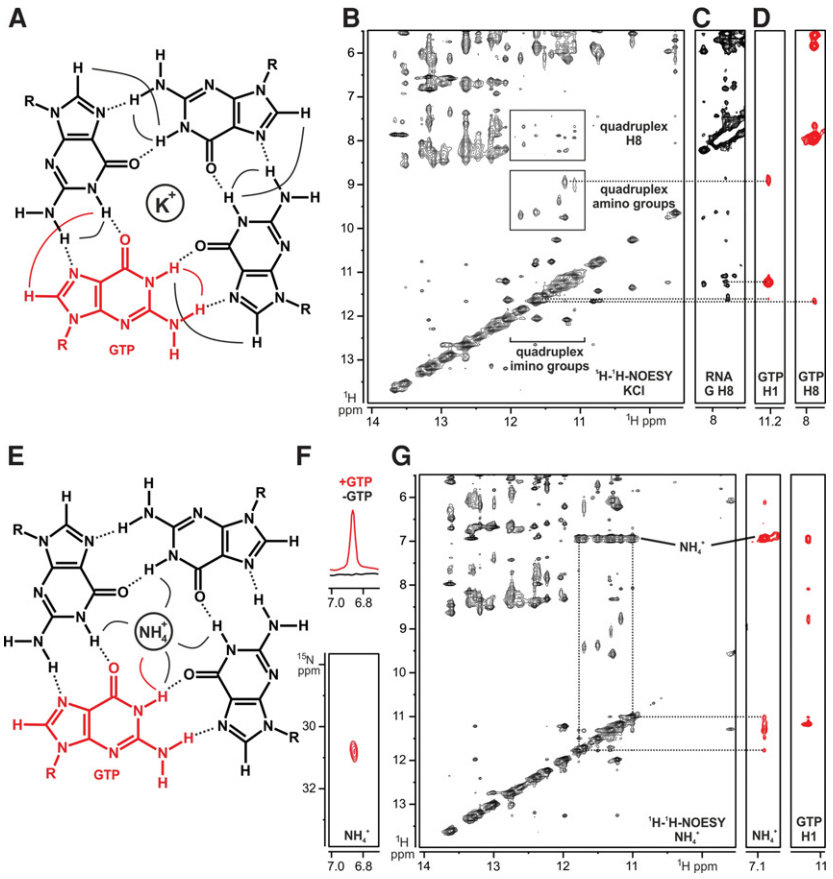

FIGURE 3. NMR evidence for the formation of an intermolecular G-quadruplex structure upon GTP binding to the class V aptamer RNA. (*A*) Structure of a single G-tetrad layer from a G-quadruplex including the bound ligand (red). Hydrogen bonds are indicated by dashed lines. Connecting lines denote expected NOE connectivities between guanine nucleotides in the quadruplex (black) including those expected for the bound GTP (red). Note that similar NOE connectivities are also observable between nucleotides in neighboring layers of a quadruplex. (*B*) 2D-^{1}H,^{1}H NOESY spectrum recorded for an unlabeled RNA bound to unlabeled GTP in potassium phosphate buffer showing NOEs involving imino protons. NOEs typical for G-quadruplex structures are highlighted by boxes and labeled accordingly. (*C*) 2D-^{1}H,^{1}H-plane from a ^{13}C-edited NOESY-HSQC spectrum recorded with a ^{15}N,^{13}C-guanine-labeled RNA bound to unlabeled GTP. This experiment allows the selective detection of NOEs from guanine H8C8 aromatic moieties to imino protons that are typical for G-quadruplexes. (*D*) Intermolecular NOEs involving the imino group (*left*) and the H8C8 group of the bound GTP as detected in either ^{15}N- (*left*) or ^{13}C-edited (*right*) NOESY-HSQC experiments recorded for samples containing ^{15}N,^{13}C-labeled ligand GTP and unlabeled RNA. (*E*) Schematic structure of a G-quadruplex tetrad bound to an ammonium ion. (*F*) The GTP–class V aptamer stably binds an ammonium ion in the presence (*top*, red) but not in the absence of bound GTP (*top*, black), as seen from 1D slices of ^{1}H,^{15}N-HSQC spectra recorded for samples containing ^{15}N-labeled ammonium chloride and unlabeled aptamer RNA or the unlabeled RNA-GTP complex. A single signal with a nitrogen chemical shift of ~30.8 ppm corresponding to the bound ammonium ion is detectable in a 2D-^{1}H,^{15}N-HSQC experiment with the RNA-GTP complex (*bottom*). Free ammonium ions are not detectable in this experiment due to the fast exchange of their protons with the bulk solvent. (*G*) The ammonium ion is located in the *center* of the G-quadruplex structure as indicated by NOEs between the ammonium ion protons and guanine imino protons seen in 2D-NOESY experiments (*left*) or in ^{15}N-edited NOESY-HSQC experiments with a sample containing ^{15}N-ammonium chloride and unlabeled RNA/GTP (*middle*). The imino proton of the bound GTP also shows an NOE to the protons of the ammonium ion as seen in a ^{15}N-edited NOESY-HSQC recorded with a sample containing ^{15}N-labeled GTP and unlabeled ammonium chloride and unlabeled RNA (*right*).

between 11 and 12 ppm (Fig. 3B,C), while other NOEs in this region report on the presence of G:U wobble base pairs as predicted by the published secondary structure (Carothers et al. 2004). The NOEs involving the ligand GTP can be selectively detected in ^{15}N- and ^{13}C-edited NOESY experiments with ^{15}N,^{13}C-labeled GTP and unlabeled RNA. Notably, the GTP imino and H8 protons show NOEs to other imino and H8 protons corroborating that the ligand GTP is actually incorporated into the quadruplex structure (Fig. 3D).

Ammonium ions often are able to replace potassium ions in G-quadruplex structures and bind in these cases between two neighboring layers of the quadruplex structure. There, they form hydrogen bonds to the O6 carbonyl groups of the eight guanines in the two layers (Hud et al. 1998, 1999; Sket et al. 2004; Podbevsek et al. 2007). Hydrogen bonding protects the ammonium protons from exchange with the protons of the bulk solvent, and in some cases an NMR signal for the bound ammonium ion can be observed in an ^{1}H,^{15}N-HSQC experiment at a signature nitrogen chemical shift of ~30 ppm when ^{15}N-labeled ammonium chloride is used (Hud et al. 1998, 1999; Podbevsek et al. 2007). Addition of ^{15}N-labeled ammonium chloride to the class V aptamer in the presence of Mg^{2+} but in the absence of GTP under our buffer conditions does not yield a detectable ^{1}H,^{15}N-HSQC signal for a bound ammonium ion (Fig. 3F). However, in the presence of GTP, a signal becomes observable for an ammonium ion protected from exchange with the solvent (Fig. 3F). Thus, GTP binding to the class V aptamer causes the formation of a binding pocket for a stably bound ammonium ion. In ^{1}H,^{1}H-NOESY or in ^{15}N-edited-NOESY experiments with ^{15}N-labeled ammonium chloride and unlabeled RNA, NOEs between the protons of the bound ammonium ion and seven to eight guanine imino protons are observable (Fig. 3G). A ^{15}N-edited NOESY-experiment with ^{15}N-labeled GTP, unlabeled RNA, and unlabeled ammonium chloride demonstrates that the imino proton of the bound GTP also shows an NOE to the bound ammonium ion (Fig. 3G). Taken together, the NOESY experiments suggest that GTP binding to the class V aptamer induces the formation of a G-quadruplex structure with two layers of guanines including the ligand

GTP and one monovalent ion bound in between the two layers.

Another characteristic feature of G-quadruplex structures is the very slow exchange of their imino protons against deuterons upon solvent exchange with D_2O (e.g., Smith and Feigon 1992). Lifetimes of imino proton signals in the order of days to weeks even at elevated temperatures have been reported for G-quadruplexes in RNA (e. g., Cheong and Moore 1992; Warner et al. 2014). In contrast, for hydrogen bonded imino protons of nucleotides in regular RNA secondary and tertiary structures, the imino proton signal normally disappears in seconds upon exchange of the solvent to D_2O (Gueron and Leroy 1995; Snoussi and Leroy 2001; Vermeulen et al. 2005). Spectra of the ^{15}N-G-labeled class V aptamer bound to ^{15}N-labeled GTP 30 min after exchange into D_2O reveal the presence of eight signals for slowly exchanging guanine imino protons in the chemical shift region from 11 to 12 ppm and one additional signal from a guanine nucleotide in a Watson-Crick base pair (Fig. 4A). Importantly, this includes the signal for the imino group of the bound GTP (Fig. 4A,B). After 4 h only four signals for RNA imino groups remain (Fig. 4B) and full exchange is observed after ~12 h. Thus, the guanine imino groups of the nucleotides forming the intermolecular G-quadruplex structure in the class V aptamer exchange significantly slower with the solvent than the other imino protons in the molecule in analogy to observations for other G-quadruplex structures. However, exchange is completed in a few hours in contrast to days or weeks as reported for some other quadruplexes. This might be due to the presence of only two G-quartets in the class V aptamer, whereas many of the other quadruplexes showing very slow imino proton exchange contain three or four G-quartets (e.g., Cheong and Moore 1992; Smith and Feigon 1992). Significantly faster imino proton exchange with rates on the order of seconds has been observed in the thrombin aptamer, which is another example for a G-quadruplex with only two G-tetrads (Mao and Gmeiner 2005). On the other hand, imino proton exchange in the class V aptamer–GTP complex occurs on a time scale similar to the reported lifetime of the RNA-ligand complex, which was previously measured in single molecule fluorescence experiments (Elenko et al. 2009). The suggestion that ligand dissociation facilitates solvent exchange is also supported by the observation that the quadruplex layer formed by three guanine residues of the RNA and the ligand GTP is apparently less stable than the layer formed by four guanine residues from the RNA (Fig. 4B).

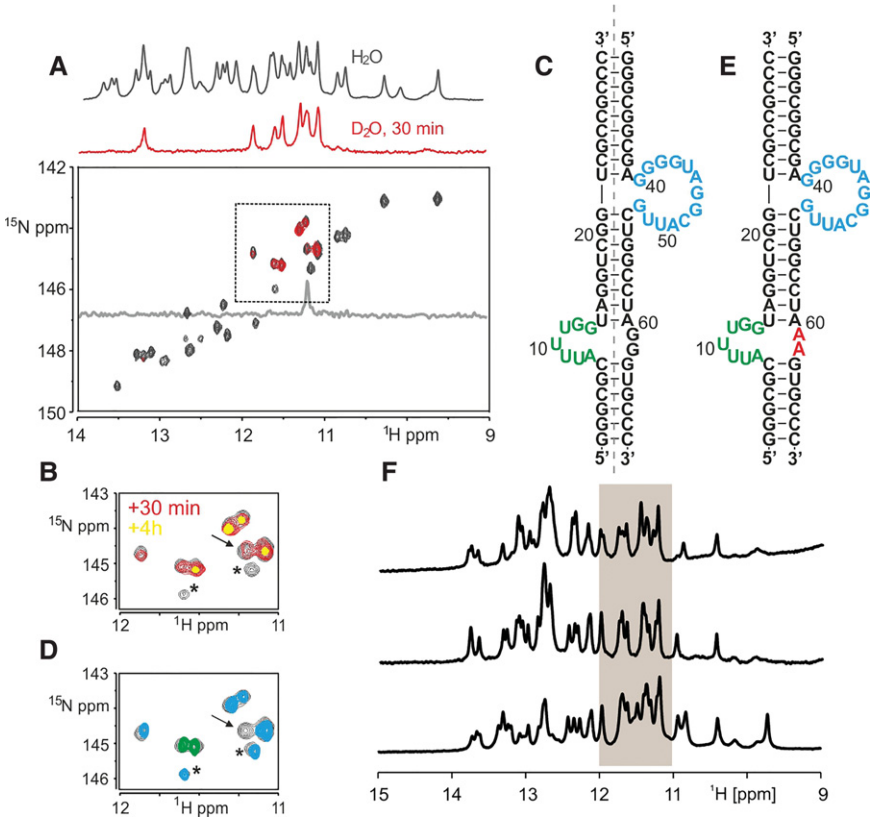

FIGURE 4. The G-quadruplex structure is formed by seven guanine nucleotides from the two asymmetric internal bulges and the bound GTP. (*A*) Comparison of 1D- ^{1}H imino proton (*top*) and ^{1}H,^{15}N-HSQC spectra (*bottom*) for the GTP-aptamer complex before (black) and 30 min after exchange of the sample into D_2O (red). A box highlights the region of guanine residues involved in G-quadruplex formation. The gray *inset* shows a 1D slice of a ^{1}H,^{15}N-HSQC spectrum recorded for a sample containing ^{15}N-GTP and unlabeled RNA 30 min after exchange into D_2O to demonstrate that the imino proton of the bound ligand is also protected against exchange with the solvent. (*B*) Overlay of the G-quadruplex imino group region of ^{1}H,^{15}N-HSQC spectra of the GTP-aptamer complex prior to (black) and 30 min (red) or 4 h (yellow) after exchange of the sample into D_2O, respectively. The signal of the imino group of the bound GTP is indicated by an arrow. The area shown corresponds to the boxed region in *A*. Resonances marked with an asterisk (*) correspond to guanine imino groups in G:U wobble base pairs. (*C*) Secondary structure of the bipartite GTP–class V aptamer construct used for strand-selective labeling experiments. A dashed line separates the 5′-strand (*left*) from the 3′-strand (*right*) of the RNA. The nucleotides of the "lower bulge" are colored in green and those of the "upper bulge" in blue. (*D*) Overlay of the G-quadruplex imino group region of ^{1}H,^{15}N-HSQC spectra of the GTP-aptamer complex with those recorded for the bipartite RNA construct ^{15}N-labeled in either the 5′-strand (green) or in the 3′-strand (blue). The imino group signal for the bound GTP (arrow) is absent in the spectra of the bipartite construct since in this experiment only unlabeled ligand was used. (*E*) Secondary structure of the bipartite GTP–class V aptamer construct with the G61A, G62A double mutation. (*F*) Comparison of 1D-^{1}H imino proton spectra of the GTP-bound form of the WT–class V aptamer (*bottom*), the bipartite aptamer construct with the WT sequence, and the G61A, G62A double mutant aptamer (*top*). Note that in comparison to the WT aptamer, the bipartite aptamer constructs both lack the apical UUCG tetraloop and therefore the diagnostic G imino proton resonance at 9.6 ppm as well as a G:U base pair in the upper stem.

According to the imino proton NOESY and $^{1}H,^{15}N$-HSQC data, the secondary structure of the class V aptamer is very similar to the original proposal published by Szostak and coworkers (Carothers et al. 2004) with two irregular asymmetric bulge elements flanked by three double-helical elements containing also G:U wobble base pairs (Fig. 1A). Thus, the G nucleotides forming the quadruplex must be located in either one or both of the two asymmetric bulge elements, which indeed contain highly conserved guanine residues. In experiments with a bipartite aptamer construct consisting of two separate strands (Fig. 4C), we labeled the guanine residues of each of the two strands separately with ^{15}N. $^{1}H,^{15}N$-HSQC spectra were recorded for differentially labeled samples bound to unlabeled GTP. These spectra revealed that two of the slowly exchanging guanine residues involved in G-quadruplex formation are located in the 5′-half of the aptamer in the "lower bulge" (Fig. 4D, green) and five of them stem from the 3′-half of the aptamer (Fig. 4D). The 3′-half of the aptamer contains "unpaired" G-residues in the upper bulge as well as in the lower bulge (G60, G61). However, a bipartite aptamer construct where G60 and G61 were mutated to A (Fig. 4E) bound GTP in a binding mode very similar to the WT aptamer (Fig. 4F; Supplemental Fig. 8). Thus, G60 and G61 do not play a role in GTP binding in agreement with their lack of conservation.

In order to pinpoint the seven G-residues involved in the formation of the intermolecular G-quadruplex with the ligand, we mutated individual G's to A's in both the lower and the upper bulge and tested GTP binding of the mutants by NMR spectroscopy and ITC experiments (Fig. 5). ^{1}H-imino proton spectra recorded for all mutants in the GTP-free state (Supplemental Fig. 9) indicated that all mutants folded into the appropriate secondary structure as judged from the presence of the UUCG-tetraloop signature signal and the amount of G and U imino proton signals with chemical shifts typical for Watson-Crick base pairs. Individual G to A mutations of either G12 or G13 in the "lower bulge" abrogated GTP binding completely (Fig. 5; Supplemental Fig. 9). Similarly, mutations of G42, G43, G46, or G47 in the "upper bulge" lead to a complete loss of GTP binding (Fig. 5; Supplemental Fig. 9). Thus, these six guanine residues are very likely candidates for taking part in the G-quadruplex formation. The G52A-mutant binds GTP similar to the WT aptamer (Supplemental Fig. 9). The G40A and the G41A point mutants still bind GTP at high concentrations but the two mutations lead to an ~1000-fold and an ~300-fold reduction in the GTP affinity of the aptamer, respectively. Together with structural considerations, this points toward G40 as the most likely candidate for the last remaining nucleotide of the G-quadruplex.

The participation of G residues located in both the "lower" and the "upper" bulge in the formation of the G-quadruplex with the GTP ligand suggests that the length but not the sequence of the central A-form helix separating these two bulges should be critical for ligand binding. According to Szostak and coworkers (Carothers et al. 2004), the sequence of the central helix is not strongly conserved. We tested the influence of shortening and extending this helix by 1 or 2 bp on GTP binding. Both the shortening and the extension of the helix by 1 bp are well tolerated by the aptamer yielding to ligand affinities similar to the WT aptamer (Fig. 6; Supplemental Fig. 10). However, a shortening of the helix by 2 bp leads to complete loss of GTP binding, whereas an extension of the helix by 2 bp reduces the GTP affinity of the aptamer 2000-fold (Fig. 6; Supplemental Fig. 10). The dependence of the GTP affinity on the length of the central helix further supports the idea that nucleotides from both the "lower" and the "upper" bulge participate in forming the GTP-binding quadruplex.

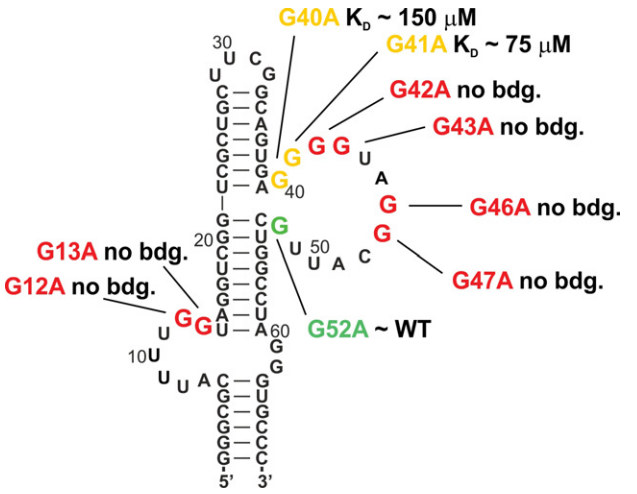

FIGURE 5. Mapping the guanine residues participating in ligand binding and intermolecular G-quadruplex formation by G to A point mutations. Shown is the secondary structure of the GTP–class V aptamer. Mutation sites that abolish binding completely are colored red (no bdg. = no binding observable even in NMR experiments with an RNA concentration of 150 μM and a 6.7-fold excess of GTP). Nucleotides where mutation reduces the K_D significantly are colored in orange, and nucleotides that can be mutated without an effect on the GTP affinity are colored green. Note that the K_D's for the G40A and G41A mutants are in the μM range. The corresponding NMR and ITC data are shown in Supplemental Figure 9.

In summary, we have shown here that the class V–GTP-binding aptamer binds GTP with a ligand-binding mode not observed in previously solved structures of either naturally occurring or artificial guanine, guanosine, or guanosine nucleotide binding RNAs. GTP is incorporated into a two-layered G-quadruplex structure formed by 7 nt of the aptamer and the ligand. The formation of this quadruplex structure is highly dependent on the identity of the monovalent cation bound in the center of the quadruplex with a strong preference for potassium ions. GTP binding through incorporation in a G-quadruplex structure is also consistent with the reported binding specificity of the class V aptamer for GTP analogs (Carothers et al. 2006b). Thus, the class V aptamer is another example of the recently growing list of

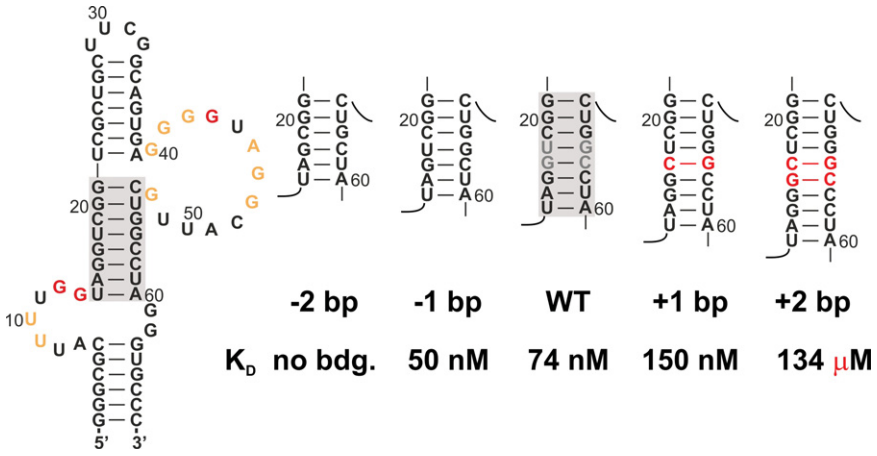

FIGURE 6. Influence of the length of the central helix on the GTP affinity of the aptamer. The secondary structure of the aptamer is shown on the *left*. A gray box highlights the central helix. The secondary structures of the shortened and extended helices are shown on the *right* with the respective K_D given *below*. Added base pairs are shown in red; gray base pairs were deleted in the shortened constructs. "No bdg." indicates that no binding is observable even in NMR experiments with an RNA concentration of 150 μM and an excess of GTP (see Supplemental Fig. 10).

functional RNAs using G-quadruple structures as a ligand-binding platform (Lauhon and Szostak 1995; Phan et al. 2011; Curtis and Liu 2013; Dolgosheina et al. 2014; Huang et al. 2014; Warner et al. 2014). However, in contrast to the genomic GTP aptamers characterized by Liu and coworkers (Curtis and Liu 2013), in the GTP–class V aptamer, G-quadruplex formation occurs only upon ligand binding. CD spectra recorded for the genomic GTP aptamers suggest that there the quadruplex structure is already preformed in the free RNA. The topology of the intermolecular G-quadruplex in the GTP–class V aptamer appears to be even more complex than the one recently reported for the spinach aptamer (Dolgosheina et al. 2014; Warner et al. 2014). In the spinach aptamer, a number of noncanonical linker residues between the guanine nucleotides lead to an unprecedented topology for the connecting loops, but all eight guanine nucleotides forming the two-layered quadruplex were located in a single internal bulge of the RNA. In the case of the class V aptamer, the RNA nucleotides contributing to quadruplex formation are located in two internal bulges separated by an A-form helical element. However, a full description of the fold of the class V aptamer–GTP complex has to await a high-resolution structure determination. Very recently, Li and coworkers reported a unique type of G-quadruplexes in genomic DNA but not RNA where one G-quartet layer misses one guanine (Li et al. 2015). These quadruplexes, which they called "guanine vacancy bearing G-quadruplexes" ("GVBQ"), bind external GMP or GTP. GMP or GTP binding fills the vacant position in the G-quartet layer missing one internal guanine residue and thereby completes this quartet and stabilizes the entire G-quadruplex. However, in their "GVBQs" the individual G-tracts forming the quadruplex were connected directly to each other by short linkers containing 3–7 nt. According to our results, the GTP–class V aptamer can be described as an RNA analog of these "guanine vacancy bearing quadruplexes" with a more complicated topology where the quadruplex is embedded in a complex tertiary structure.

MATERIALS AND METHODS

Class V–GTP aptamer RNA was prepared by in vitro transcription using T7 RNA polymerase according to standard protocols previously described in detail (Duchardt-Ferner et al. 2010). For the transcription of the full-length GTP aptamer, linearized plasmid was used as a template. Split GTP aptamer and mutant constructs were transcribed from synthetic DNA oligonucleotides (Eurofins Genomics) that were annealed to a T7-promotor primer (Milligan et al. 1987). All RNAs were purified by denaturing urea PAGE. For annealing split RNA constructs, single strands at a concentration of 100 μM were heated to 90°C for 1 min in a buffer consisting of 25 mM KPO_4, 25 mM KCl, 2 mM $MgCl_2$, 1 mM GTP, pH 6.3, followed by cooling to room temperature over ~5 min. All NMR measurements were performed using standard pulse sequences and Bruker Avance 600, 700, 800, 900, and 950 MHz spectrometers equipped with cryogenic probes at 10°C or 20°C. Buffers for NMR measurements were K-phosphate buffer (25 mM KPO_4, 25 mM KCl, 2–5 mM $MgCl_2$, pH 6.3), Na-phosphate buffer (25 mM $NaPO_4$, 25 mM NaCl, 2–5 mM $MgCl_2$, pH 6.3), or NH_4Cl buffer (50 mM Bis-Tris/HCl, 50 mM NH_4Cl, 5 mM $MgCl_2$, pH 6.3) unless noted otherwise. For the H/D-exchange experiments, NMR samples prepared in aqueous buffer were lyophilized and subsequently dissolved in an equivalent volume of D_2O.

ITC measurements were performed at 20°C in 2 mM $MgCl_2$, 50 mM Bis-Tris/HCl, pH 6.5, and 50 mM of the respective salt (KCl, NaCl, LiCl, $TlNO_3$, or NH_4Cl) using a MicroCal iTC200 calorimeter (Malvern Instruments). For measurements involving $TlNO_3$, Bis-Tris/AcOH, pH 6.5, and Mg acetate were used instead of Bis-Tris/HCl and $MgCl_2$ due to the extremely low solubility of thallium chloride. Twenty to 48 μM of GTP aptamer were titrated with 200–350 μM GTP, power curves were integrated and corrected for a titration of GTP into buffer. For GTP aptamer mutants with K_D's larger than the WT, both the RNA and the GTP concentrations were increased accordingly. The binding isotherms were fitted in Origin 7 using the one-site binding model provided by Microcal.

SUPPLEMENTAL MATERIAL

Supplemental material is available for this article.

ACKNOWLEDGMENTS

This work was supported by the Aventis Foundation, the Center of Biomolecular Magnetic Resonance (BMRZ), and the Deutsche Forschungsgemeinschaft (WO 901/1-1 and project B10 of the CRC [SFB] 902 "Molecular Principles of RNA-based

Regulation"). We are grateful to E. Duchardt-Ferner and members of the Wöhnert group for helpful discussions, to K. Yacoub for help with sample preparations, and to P.J. Harvey for continuous encouragement.

Received August 26, 2016; accepted August 31, 2016.

REFERENCES

Adams PL, Stahley MR, Kosek AB, Wang J, Strobel SA. 2004. Crystal structure of a self-splicing group I intron with both exons. *Nature* **430:** 45–50.

Basu S, Rambo RP, Strauss-Soukup J, Cate JH, Ferré-D'Amaré AR, Strobel SA, Doudna JA. 1998. A specific monovalent metal ion integral to the AA platform of the RNA tetraloop receptor. *Nat Struct Biol* **5:** 986–992.

Basu S, Szewczak A, Cocco M, Strobel SA. 2000. Direct detection of monovalent metal ion binding to a DNA G-quartet by ^{205}Tl NMR. *J Am Chem Soc* **122:** 3240–3241.

Batey RT, Gilbert SD, Montange RK. 2004. Structure of a natural guanine-responsive riboswitch complexed with the metabolite hypoxanthine. *Nature* **432:** 411–415.

Carothers JM, Oestreich SC, Davis JH, Szostak JW. 2004. Informational complexity and functional activity of RNA structures. *J Am Chem Soc* **126:** 5130–5137.

Carothers JM, Davis JH, Chou JH, Szostak JW. 2006a. Solution structure of an informationally complex high-affinity RNA aptamer to GTP. *RNA* **12:** 567–579.

Carothers JM, Oestreich SC, Szostak JW. 2006b. Aptamers selected for higher-affinity binding are not more specific for the target ligand. *J Am Chem Soc* **128:** 7929–7937.

Cech TR, Zaug AJ, Grabowski PJ. 1981. In vitro splicing of the ribosomal RNA precursor of tetrahymena: involvement of a guanosine nucleotide in the excision of the intervening sequence. *Cell* **27:** 487–496.

Cheong C, Moore PB. 1992. Solution structure of an unusually stable RNA tetraplex containing G- and U-Quartet structures. *Biochemistry* **31:** 8406–8414.

Conn GL, Gittis AG, Lattman EE, Misra VK, Draper DE. 2002. A compact RNA tertiary structure contains a buried backbone-K+ complex. *J Mol Biol* **318:** 963–973.

Curtis EA, Liu DR. 2013. Discovery of widespread GTP-binding motifs in genomic DNA and RNA. *Chem Biol* **20:** 521–532.

Davis JH, Szostak JW. 2002. Isolation of high-affinity GTP aptamers from partially structured RNA libraries. *Proc Natl Acad Sci* **99:** 11616–11621.

Dingley AJ, Grzesiek S. 1998. Direct observation of hydrogen bonds in nucleic acid base pairs by internucleotide $^{2}J_{NN}$ couplings. *J Am Chem Soc* **120:** 1601–1602.

Dolgosheina EV, Jeng SC, Panchapakesan SS, Cojocaru R, Chen PS, Wilson PD, Hawkins N, Wiggins PA, Unrau PJ. 2014. RNA mango aptamer-fluorophore: a bright, high-affinity complex for RNA labeling and tracking. *ACS Chem Biol* **9:** 2412–2420.

Duchardt-Ferner E, Weigand JE, Ohlenschläger O, Schmidtke SR, Suess B, Wöhnert J. 2010. Highly modular structure and ligand binding by conformational capture in a minimalistic riboswitch. *Angew Chem Int Ed Engl* **49:** 6216–6219.

Edwards AL, Batey RT. 2009. A structural basis for the recognition of 2′-deoxyguanosine by the purine riboswitch. *J Mol Biol* **385:** 938–948.

Elenko MP, Szostak JW, van Oijen AM. 2009. Single-molecule imaging of an in vitro-evolved RNA aptamer reveals homogeneous ligand binding kinetics. *J Am Chem Soc* **131:** 9866–9867.

Fürtig B, Richter C, Wöhnert J, Schwalbe H. 2003. NMR spectroscopy of RNA. *Chembiochem* **4:** 936–962.

Gill ML, Strobel SA, Loria JP. 2005. ^{205}Tl NMR methods for the characterization of monovalent cation binding to nucleic acids. *J Am Chem Soc* **127:** 16723–16732.

Gill ML, Strobel SA, Loria JP. 2006. Crystallization and characterization of the thallium form of the *Oxytricha nova* G-quadruplex. *Nucleic Acids Res* **34:** 4506–4514.

Gueron M, Leroy JL. 1995. Studies of base pair kinetics by NMR measurement of proton exchange. *Methods Enzymol* **261:** 383–413.

Huang Z, Szostak JW. 2003. Evolution of aptamers with a new specificity and new secondary structures from an ATP aptamer. *RNA* **9:** 1456–1463.

Huang H, Suslov NB, Li NS, Shelke SA, Evans ME, Koldobskaya Y, Rice PA, Piccirilli JA. 2014. A G-quadruplex-containing RNA activates fluorescence in a GFP-like fluorophore. *Nat Chem Biol* **10:** 686–691.

Hud NV, Schultze P, Feigon J. 1998. Ammonium ion as an NMR probe for monovalent cation coordination sites of DNA quadruplexes. *J Am Chem Soc* **120:** 6403–6404.

Hud NV, Schultze P, Sklenár V, Feigon J. 1999. Binding sites and dynamics of ammonium ions in a telomere repeat DNA quadruplex. *J Mol Biol* **285:** 233–243.

Jin RZ, Breslauer KJ, Jones RA, Gaffney BL. 1990. Tetraplex formation of a guanine-containing nonameric DNA fragment. *Science* **250:** 543–546.

Jin R, Gaffney BL, Wang C, Jones RA, Breslauer KJ. 1992. Thermodynamics and structure of a DNA tetraplex: a spectroscopic and calorimetric study of the tetramolecular complexes of d(TG_3T) and d($TG_3T_2G_3T$). *Proc Natl Acad Sci* **89:** 8832–8836.

Kim J, Cheong C, Moore PB. 1991. Tetramerization of an RNA oligonucleotide containing a GGGG sequence. *Nature* **351:** 331–332.

Kim JN, Roth A, Breaker RR. 2007. Guanine riboswitch variants from *Mesoplasma florum* selectively recognize 2′-deoxyguanosine. *Proc Natl Acad Sci* **104:** 16092–16097.

Kulshina N, Baird NJ, Ferré-D'Amaré AR. 2009. Recognition of the bacterial second messenger cyclic diguanylate by its cognate riboswitch. *Nat Struct Mol Biol* **16:** 1212–1217.

Lauhon CT, Szostak JW. 1995. RNA aptamers that bind flavin and nicotinamide redox cofactors. *J Am Chem Soc* **117:** 1246–1257.

Lee ER, Baker JL, Weinberg Z, Sudarsan N, Breaker RR. 2010. An allosteric self-splicing ribozyme triggered by a bacterial second messenger. *Science* **329:** 845–848.

Li XM, Zheng KW, Zhang JY, Liu HH, He YD, Yuan BF, Hao YH, Tan Z. 2015. Guanine-vacancy-bearing G-quadruplexes responsive to guanine derivatives. *Proc Natl Acad Sci* **112:** 14581–14586.

Macaya RF, Schultze P, Smith FW, Roe JA, Feigon J. 1993. Thrombin-binding DNA aptamer forms a unimolecular quadruplex structure in solution. *Proc Natl Acad Sci* **90:** 3745–3749.

Mandal M, Boese B, Barrick JE, Winkler WC, Breaker RR. 2003. Riboswitches control fundamental biochemical pathways in *Bacillus subtilis* and other bacteria. *Cell* **113:** 577–586.

Mao X, Gmeiner WH. 2005. NMR study of the folding–unfolding mechanism for the thrombin-binding DNA aptamer d(GGTTGGTGTGGTTGG). *Biophys Chem* **113:** 155–160.

Milligan JF, Groebe DR, Witherell GW, Uhlenbeck OC. 1987. Oligoribonucleotide synthesis using T7 RNA polymerase and synthetic DNA templates. *Nucleic Acids Res* **15:** 8783–8798.

Noeske J, Richter C, Grundl MA, Nasiri HR, Schwalbe H, Wöhnert J. 2005. An intermolecular base triple as the basis of ligand specificity and affinity in the guanine and adenine sensing riboswitch RNAs. *Proc Natl Acad Sci* **102:** 1372–1377.

Phan AT, Kuryavyi V, Darnell JC, Serganov A, Majumdar A, Ilin S, Raslin T, Polonskaia A, Chen C, Clain D, et al. 2011. Structure-function studies of FMRP RGG peptide recognition of an RNA duplex-quadruplex junction. *Nat Struct Mol Biol* **18:** 796–804.

Pikovskaya O, Polonskaia A, Patel DJ, Serganov A. 2011. Structural principles of nucleoside selectivity in a 2′-deoxyguanosine riboswitch. *Nat Chem Biol* **7:** 748–755.

Podbevsek P, Hud NV, Plavec J. 2007. NMR evaluation of ammonium ion movement within a unimolecular G-quadruplex in solution. *Nucleic Acids Res* **35:** 2554–2563.

Serganov A, Yuan YR, Pikovskaya O, Polonskaia A, Malinina L, Phan AT, Hobartner C, Micura R, Breaker RR, Patel DJ. 2004.

Structural basis for discriminative regulation of gene expression by adenine- and guanine-sensing mRNAs. *Chem Biol* **11:** 1729–1741.

Sket P, Crnugelj M, Kozminski W, Plavec J. 2004. $^{15}NH_4^+$ ion movement inside $d(G_4T_4G_4)_2$ G-quadruplex is accelerated in the presence of smaller Na^+ ions. *Org Biomol Chem* **2:** 1970–1973.

Smith FW, Feigon J. 1992. Quadruplex structure of *Oxytricha* telomeric DNA oligonucleotides. *Nature* **356:** 164–168.

Smith KD, Lipchock SV, Ames TD, Wang J, Breaker RR, Strobel SA. 2009. Structural basis of ligand binding by a c-di-GMP riboswitch. *Nat Mol Struct Biol* **16:** 1218–1223.

Smith KD, Shanahan CA, Moore EL, Simon AC, Strobel SA. 2011. Structural basis of differential ligand recognition by two classes of bis-(3′-5′)-cyclic dimeric guanosine monophosphate-binding riboswitches. *Proc Natl Acad Sci* **108:** 7757–7762.

Snoussi K, Leroy JL. 2001. Imino proton exchange and base pair kinetics in RNA duplexes. *Biochemistry* **40:** 8898–8904.

Sudarsan N, Lee ER, Weinberg Z, Moy RH, Kim JN, Link KH, Breaker RR. 2008. Riboswitches in eubacteria sense the second messenger cyclic di-GMP. *Science* **321:** 411–413.

Varani G, Cheong C, Tinoco I Jr. 1991. Structure of an unusually stable RNA hairpin. *Biochemistry* **30:** 3280–3289.

Vermeulen A, McCallum SA, Pardi A. 2005. Comparison of the global structure and dynamics of native and unmodified $tRNA^{Val}$. *Biochemistry* **44:** 6024–6033.

Wacker A, Buck J, Mathieu D, Richter C, Wöhnert J, Schwalbe H. 2011. Structure and dynamics of the deoxyguanosine-sensing riboswitch studied by NMR-spectroscopy. *Nucleic Acids Res* **39:** 6802–6812.

Wang Y, de los Santos C, Gao XO, Greene K, Live D, Patel DJ. 1991a. Multinuclear nuclear magnetic resonance studies of Na cation-stabilized complex formed by d(G-G-T-T-T-T-C-G-G) in solution. Implications for G-tetrad structures. *J Mol Biol* **222:** 819–832.

Wang Y, Jin R, Gaffney B, Jones RA, Breslauer KJ. 1991b. Characterization by ^1H NMR of glycosidic conformations in the tetramolecular complex formed by d(GGTTTTTGG). *Nucleic Acids Res* **19:** 4619–4622.

Wang YX, Lu M, Draper DE. 1993. Specific ammonium ion requirement for functional ribosomal RNA tertiary structure. *Biochemistry* **32:** 12279–12282.

Warner KD, Chen MC, Song W, Strack RL, Thorn A, Jaffrey SR, Ferré-D'Amaré AR. 2014. Structural basis for activity of highly efficient RNA mimics of green fluorescent protein. *Nat Struct Mol Biol* **21:** 658–663.

Wöhnert J, Dingley AJ, Stoldt M, Görlach M, Grzesiek S, Brown LR. 1999. Direct identification of NH···N hydrogen bonds in non-canonical base pairs of RNA by NMR spectroscopy. *Nucleic Acids Res* **27:** 3104–3110.